Journal of Nanomaterials & Molecular Nanotechnology

Research Article

A SCITECHNOL JOURNAL

Synthesis of Metal-Oxide (Al_2O_3) Nanoparticles by using Autoclave for the Efficient Absorption of Heavy Metal Ions

Rabeya Akter Rabu[1], Nasrin Jewena[2*],Sujan Kumar Das[1], Jahirul Islam Khandaker[1], and Farid Ahmed[1]

Abstract

Metal-oxide (Al2O3) nanoparticles were synthesized by hydrothermal method within a self-designed stainless-steel autoclave, sealed, and heated at 140°C for 48 hours. The X-ray Diffraction (XRD) analysis confirmed characteristic Al2O3 crystal peaks at diffraction angles near 25.8°C, 35.1°C, 37°C, and 41°C (2θ). XRD analysis also measured the average crystallite size of 30 nm for the as-synthesized γ-Al2O3 nanoparticles. The absorption bands of Al2O3 stretching were confirmed at 515 cm-1 and 736 cm-1 through Fourier Transform Infrared Spectroscopy (FT-IR) analysis. The UV-Vis spectroscopy identified a strong absorption peak at 267 nm for (Al2O3) nanoparticles. The bandgap was calculated at 5.34 eV from the Tauc plot that was much lower than that of the bulk counterpart due to the existence of defect states located in the band gap region. The performance of the removal of heavy metal ions was examined by a batch-adsorption technique. The removal of lead and cadmium ions from aqueous solutions was rapid and efficient. It was found to be 98% and 85% for Pb(II) ion and Cd(II) ion respectively. The adsorption isotherms were determined by using Langmuir isotherm and the maximum absorption capacity was identified as 6.3 mg/g and 1.8 mg/g for Pb(II) ion and Cd(II) ion respectively for 10 ppm solution respectively.

Keywords

Nanoparticles; Alumina (Al2O3); Autoclave; Band gap; Adsorption; Langmuir isotherm

Introduction

Nanoparticle synthesis is currently an arena of diligent scientific research, by virtue of a wide range of potential functions and operations in biomedical, optical, electric fields, medicine, imaging, computing, chemical catalysis, materials synthesis, and wastewater treatment [1]. Nanomaterials largely show unique and significant variation in physical and chemical properties when the bulk materials transform into nanomaterials with a similar chemical composition [2]. There is a dire need for new materials with a special combination of properties to accommodate the increasing needs of modern technology. Metal Oxides Nanoparticles (MONPs) have become an indispensable tool in modern science and technology because of their unique properties and wide range of applications in electronics, environmental conversion, solar cells, medicine, biosensors, etc. [3]. Among MONPs, alumina (Al_2O_3) is an important candidate having various phases of γ, θ, and . The γ-phase is formed at a high calcination temperature of about 600°C [4]. The γ-Al_2O_3 nanoparticles exhibit strong heavy metal adsorption activity which has explored their potential applications in water purification along with other industrial [5]. The challenge of providing and ensuring clean and fresh water is rapidly growing as the world's population increases, there are currently more than 0.78 billion people around the world who do not have access to safe water resources [6]. The amount over 0.006 mg/L lead present in water causes damage to the fetal brain, diseases of the kidneys, circulatory system, and nervous system [7] and the amount over 0.006 mg/L cadmium present in water causes damage to the fetal brain, diseases of the kidneys, circulatory system and nervous system [7]. Gamma-alumina nanoparticles are favorable materials as adsorbents as they have mechanical strength, large specific surface area, high adsorption capacity, and low-temperature modification [8].

In the current studies, a simple and cost-effective hydrothermal method was employed to synthesis gamma-alumina nanoparticles from Aluminium sulfate hydrate within autoclave [9], and then characterized for heavy metal ions removal. The synthesized Al_2O_3 nanoparticles were calcined at 600°C for 6 hours. Then the properties and characteristics of Alumina nanoparticles were studied and discussed. Finally, the as-synthesized nano γ-Al_2O_3 was used for the adsorption of heavy metal ions Pb(II) and Cd(II) from aqueous solution under batch conditions and adsorption process [10].

Materials and Methods

All the chemicals and reagents used in this study were of analytical grade and commercially pure. The essential chemicals used in the experiment were Aluminium sulfate octadecahydrate ($Al_2(SO_4)_3{\cdot}18H_2O$) having a purity of 99% (450308, Sigma-Aldrich), polyethylene glycol ($C_2H_6O_2$) with a purity of 98.5% (Loba Chemie Pvt. Ltd), Ammonia (NH_3) having a purity of 99.99% (Loba Chemie Pvt. Ltd), Ethanol (C_2H_5OH) having a purity of 98%, Cadmium sulfate ($CdSO_4$) having purity of 99.99% (Loba Chemie Pvt. Ltd) and distilled water (H_2O).

Synthesis of γ-Al_2O_3 NPs

Aluminium sulfate ($Al_2(SO_4)_3{\cdot}18H_2O$) and polyethylene glycol were dissolved in 100 mL distilled water. Then the obtained solution was continuously stirred for 1 hour at room temperature in a magnetic stirrer [10]. A quantity of ammonia (25%) was added at a constant rate into the solution which gave rise to milky precipitates at pH=9. The solution was placed in a stainless-steel autoclave (Figure 1) and was sealed and heated at 140 ° C for 48 hours. The obtained product was dried at 100°C for 1h and calcined at 600°C for 6 hours (Figure 2).

Characterization techniques

The structure of the synthesized nanoparticles, optical properties, and electric properties had been characterized by advanced techniques such as XRD, UV-Vis, and FT-IR. The powder X-ray

***Corresponding author:** Nasrin Jewena, Department of Chemistry, Jahangirnagar University, Savar, Dhaka, 1342, Bangladesh, E-mail: nasrin28ju@juniv.edu

Received: December 04, 2020 **Accepted:** December 14, 2020 **Published:** December 22, 2020

diffraction experiments were carried out by the GNR explorer series X-ray diffractometer. Monochromatic CuKα radiations were used as a source of 40 kV/35 mA power and the pattern was recorded in the 2θ range from 2=10° to 2θ=50°. Finally, the as-synthesized nano γ-Al_2O_3 was used for the adsorption of heavy metal ion, Cd(II), and Pb(II) which was investigated by Atomic absorption spectroscopy.

Adsorption studies

10 ppm Cd(II) and Pb(II) ion solution was prepared using double distilled water and 0.1 gm, 0.03 gm, and 0.07 gm synthesized γ-Al_2O_3 was added to the solution at a constant rate [11]. 10 ml sample was withdrawn at 1 minutes, 3 minutes, 5 minutes, 10 minutes, 30 minutes, 60 minutes, 90 minutes, 120 minutes, 150 minutes, 180 minutes time interval. A basic assumption in the Langmuir theory is that sorption takes place at specific homogeneous sites within the adsorbent. The most widely used equation [12] that is valid for monolayer adsorption and the linear form of the Langmuir model is given by,

Figure 1: Autoclave used in the experiment.

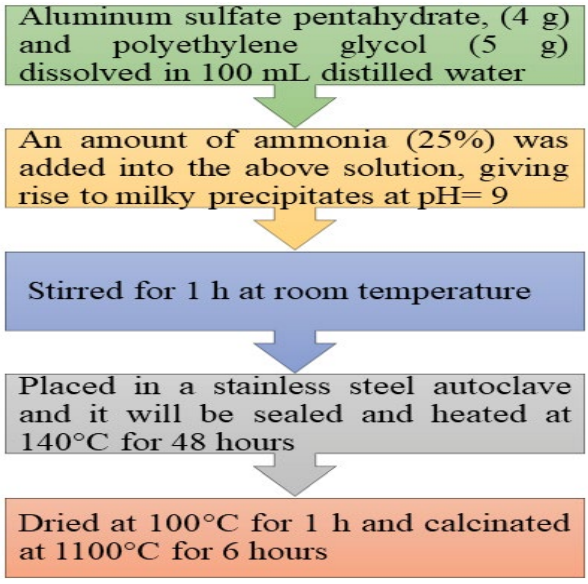

Figure 2: Flow chart for the synthesis of γ-Al_2O_3 powder by hydrothermal method.

$$\frac{c_e}{q_e} = \frac{c_e}{q_{\max}} + \frac{K_L}{q_{\max}} \quad (1)$$

Where q_{max} (mg g^{-1}) was the maximum adsorption capacity at monolayer, C_e was the concentration of ions at equilibrium, q_e was the adsorption capacity at equilibrium (mg g^{-1}) and R_L was the Langmuir constant representing the affinity of binding sites (L/mg) [13].

A linear plot of C_e/q_e versus C_e gives the values of q_{max} and K_L [14]. One of the essential characteristics of the Langmuir isotherm was a dimensionless constant of separation factor or equilibrium parameter, R_L, which is given by,

$$R_L = \frac{1}{1 + K_L C_o} \quad (2)$$

Where K_L was the Langmuir constant and c_o as the initial concentration of dyes. If R_L values were between 0 and 1 then it indicates favorable adsorption. The amount of adsorbed heavy metal onto the adsorbent material per unit mass of adsorbent was defined by the following equation [15].

$$q_e = \frac{(C_o - C_e)V}{W} \quad (3)$$

Where ions uptake at equilibrium, q_e (mg/g), c_o and c_e (mg/L) were the initial and equilibrium concentrations of the ion solutions, respectively. V(L) identifies the volume of the solution, and W(g) indicates the mass of adsorbent.

Also, percentage of removal (%*R*) of ions was calculated from the following equation [15]

$$\%R = \frac{C_o - C_e \times 100}{C_o} \quad (4)$$

Result and Discussion

XRD analysis

The X-ray Diffraction (XRD) analysis confirmed the characteristic Al_2O_3 crystal peaks at diffraction angles near 25.8°C, 35.1°C, 37°C, and 41°C (2θ). XRD analysis also measured the crystallite size of γ-Al_2O_3 nanoparticles synthesized by the hydrothermal method. The average crystallite sizes of the samples were found 30 nm which was measured from the Full Width at Half Maximum (FWHM) of the peaks (β) using the Debye Scherrer formula [16],

$$D = \frac{K\lambda}{\beta \cos\theta} \quad (5)$$

Where D is the crystal size, K is the shape factor, λ is the X-ray wavelength and θ is the Bragg angle. The peaks in Figure 3 strongly specify the formation of crystalline nano-sized γ-Al_2O_3 powders [17]. γ-Al_2O_3 is a dual-phase system, consisting of cubic γ-Al_2O_3 and tetragonal γ-Al_2O_3 [18]. The main XRD peaks of the γ-Alumina phase were observed and shown in Table 1. The other peaks in the graph indicate the presence of alpha alumina nanoparticles

According to Bragg's law [1] the interference is constructive when the following condition is accomplished:

$$D = \frac{K\lambda}{\beta \cos\theta} \quad (6)$$

Where n is a whole number, d is the distance between planes inside the crystal grid.

FTIR analysis

FT-IR spectroscopy is convenient in evaluating the absorption of IR radiations by a sample. The evaluation of the IR spectrum contains the connection of the absorption bands (vibrational bands) and the chemical compounds in the sample [19]. The FTIR spectrum of synthesized aluminium oxide nanoparticles is shown in Figure 4. The peaks at 515 cm^{-1} and 736 cm^{-1} are assigned to the aluminium oxide stretching [20]. The peaks at 3400 cm^{-1} to 3600 cm^{-1} are assigned to the bending and stretching vibration mode of a water molecule. The band at 1182 cm^{-1} was due to the C=O stretching mode and this bond had been possibly formed due to the reaction of ammonia from the precursor [21].

UV-Vis spectroscopy

UV-visible absorption spectral study assisted in understanding the electronic structure of the optical bandgap of the material. Figure 5 shows the UV-visible absorption spectra of Al_2O_3 NPs suspended in deionized water by sonication for 30 min [22]. A strong absorption was observed near 267 nm that identified the presence of Al_2O_3 NPs. The absorbance was proportional to the number density and hence it was used to measure the formation rate and the stability of alumina nanoparticles during the synthesis [23].

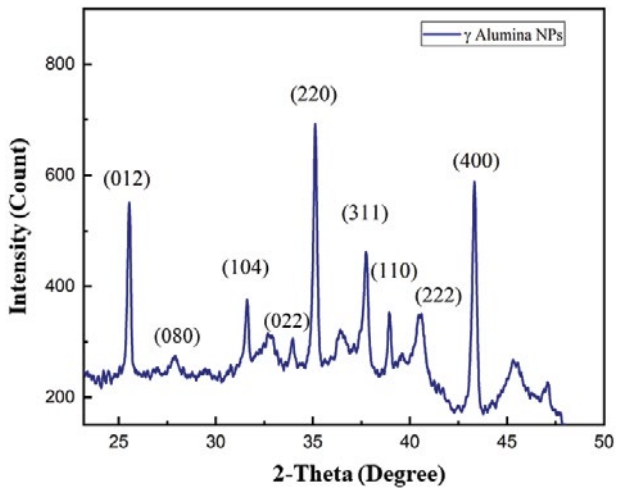

Figure 3: XRD pattern of gamma alumina NPs calcined at 600 ° C.

Table 1: X-ray diffraction patterns of alumina nanopowder and the standard 2θ with the corresponding d-spacing.

Standard 2θ [20]	Observed 2θ (degree)	h k l	d-spacing (nm)
25.5 (γ)	25.8	0 1 2	0.48
32.1 (γ)	35.1	2 2 0	0.27
34.7 (γ)	37.3	2 2 2	0.26
45.9 (γ)	43.6	4 0 0	0.19

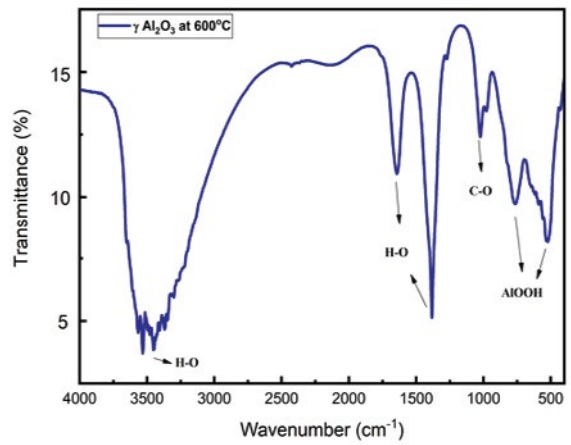

Figure 4: FTIR spectrum of gamma aluminium oxide NPs.

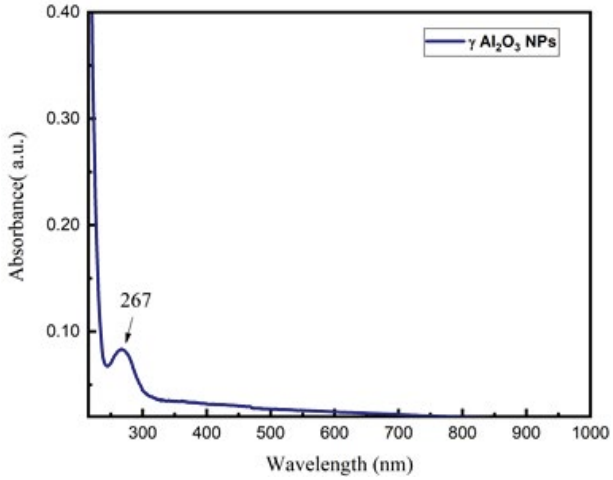

Figure 5: UV-Vis spectrum of gamma aluminium oxide NPs.

Bandgap energy

The bandgap of the nanoparticles was calculated from the Tauc plot. The strong absorption band was found at a low wavelength near 267 nm correspond to 5.34 eV. Bulk aluminium oxide was an insulator with a wide bandgap between 8.7 eV and 9.4 eV, but in the case of nanoparticles due to the defect levels located in the bandgap, it was decreased to 5.34 eV [21,24] (Figure 6).

Adsorption Isotherm

Effect of adsorbent dose: The results of the experiments with varying adsorbent concentrations are shown in Figure 7 which illustrated that the adsorption was highly dependent on the adsorbent dose. An increase in the adsorbent dose, from 0.03 mg to 0.07 mg, increases the removal of Pb(II) ions from 94% to 97% which was calculated by equation (4). It is obvious that the removal of Pb(II) ions is not increased considerably when the adsorbent dose was higher than 0.07 mg. Thus, the optimum dosage for adsorption of Pb(II) ions is found to be 0.07 mg for 10 ppm lead ion solution as all active sites

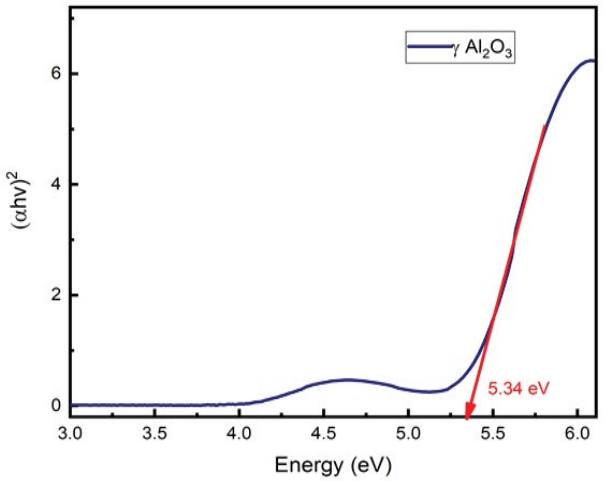

Figure 6: Bandgap energy of gamma aluminium oxide NPs.

on the adsorbent surface are then engaged and growth in adsorbent dosage do not provide higher uptake of Pb(II) ions [22].

The effective removal of the heavy metal ions was mainly dependent on the ratio of adsorbent dose to the concentration of metal ions, which was of course a compromise with the desired cost-effective retention percentage. As time progressed, these sites became more occupied and the occupation of the remaining vacant surface sites became more difficult because of repulsive forces between the metal ions on the solid and the liquid phases [25]. The maximum capacity was identified as 6.3 mg/g for lead ion adsorption by equation (1) and shown in Table 2. In case of cadmium ion removal, observing Figure 8 (b), an increase in the adsorbent dose from 0.6 mg to 0.9 mg, increases the removal of cadmium (II) ions from 92% to 97.52% respectively which was calculated by equation (4). It is obvious that the removal of cadmium (II) ions was not increased considerably when the adsorbent dose was higher than 0.9 mg.

Thus, the optimum dosage for adsorption of cadmium (II) ions is found to be 0.9 mg for 10 ppm cadmium ion solution as all active sites

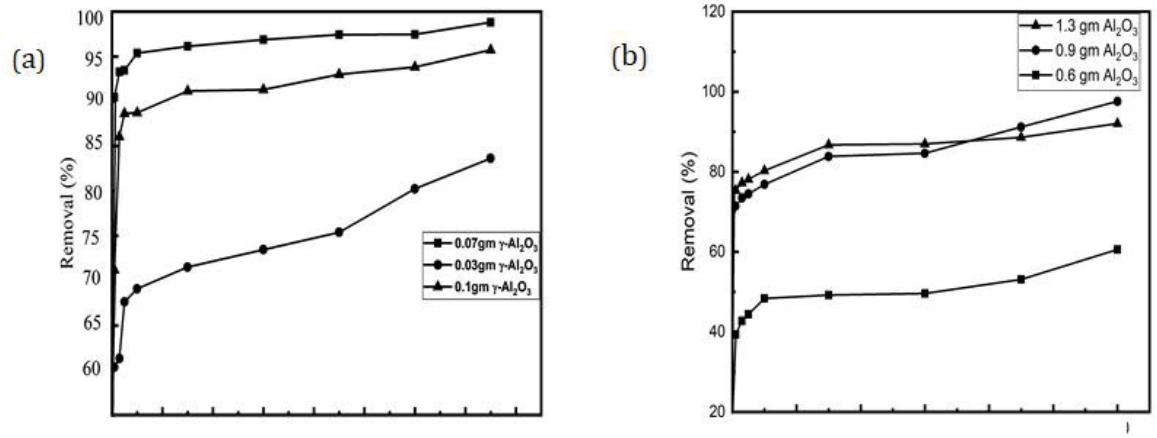

Figure 7: Effect of adsorbent weight (gamma alumina NPs) (g) on the (a) percentage removal of lead; (b) cadmium (Cd) removal by nano γ-alumina at a solution concentration of 10ppm

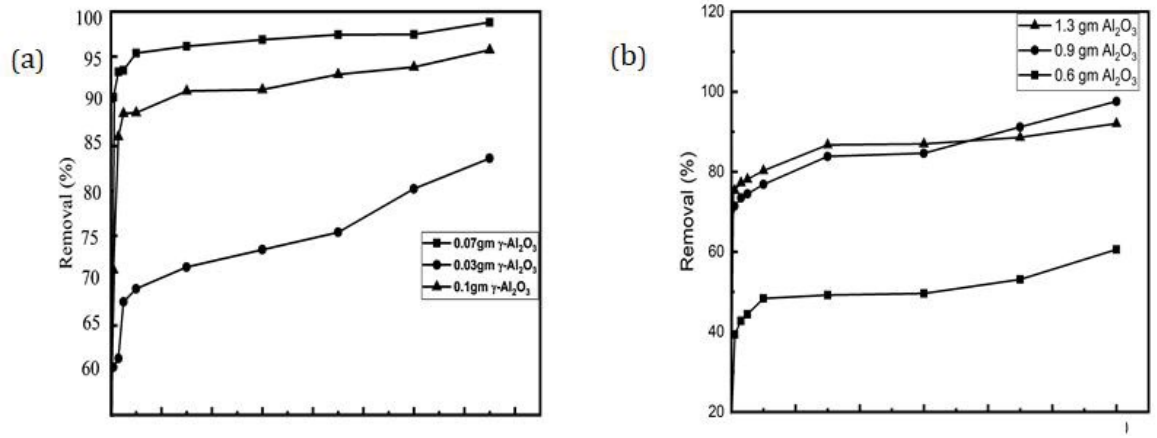

Figure 8: Langmuir isotherm for (a) lead adsorption onto w=0.07gm nano γ-Al_2O_3 powder ;(b) langmuir isotherm data of Cadmium (II) ions adsorption onto nano γ-alumina of 0.9gm at a temperature of (28 ° C).

Table 2: Isotherm modeling results related to the Pb(II) and Cd(II) adsorption onto nano alumina.

Heavy metal ion	Amount of adsorbent γ-Al_2O_3 (gm)	Concentration (ppm)	Langmuir isotherm parameters	
Lead ion	0.07	10	q_m	6.3 (mg/g)
			R_L	0.86 (L/mg)
			R^2	0.7066
Cadmium ion	0.9	10	q_m	1.8 (mg/g)
			R_L	0.96 (L/mg)
			R^2	0.832

on the adsorbent surface are then engaged and growth in adsorbent dosage do not provide higher uptake of cadmium (II) ions. The effective removal of the heavy metal ions was mainly dependent on the ratio of adsorbent dose to the concentration of metal ions, which was of course a compromise with the desired cost-effective retention percentage. From Figure 8 we can see that the adsorption isotherms for Pb(II) and Cd(II) had exhibited a good fitting to the Langmuir model as the RL values are between 0 and 1 and it indicates favourable adsorption.

Effect of contact time: During the initial stage of adsorption, there is a rapid uptake of metal ions which slowed down after 30 min of contact time. Equilibrium was reached within 60 min of contact time. Initially, a large number of vacant surface sites are available for adsorption which gets saturated gradually. Once the site of the sorbent is filled, no further adsorption can take place on the sites [26]. The adsorption efficiency depends on the surface area of the adsorbent. At the first 30 min, the increment in adsorption capacity was very fast which can be explained by the increasing number of active metal-binding sites on the adsorbent surface at the beginning, which would lead to an increasing concentration gradient between adsorbate in the solution and on the adsorbent surface [27].

Conclusion

In the current studies, metal-oxide (Al_2O_3) nanoparticles were synthesized by using an easy, cheap, and rapid green method namely hydrothermal method with the assistance of self-designed stainless-steel autoclave, sealed and heated at 140°C for 48 hours. The X-ray Diffraction (XRD) analysis confirmed characteristic Al_2O_3 crystal peaks at diffraction angles near 25.8°C, 35.1C, 37°C and 41C (2θ). XRD analysis also measured the average crystallite size of 30 nm for the as-synthesized γ-Al_2O_3 nanoparticles. The absorption bands of Al_2O_3 stretching were confirmed at 515 cm^{-1} and 736 cm^{-1} through Fourier Transform Infrared Spectroscopy (FT-IR) analysis. The UV-Vis spectroscopy identified a strong absorption peak at 267 nm for (Al_2O_3) nanoparticles. The band gap was calculated 5.34 eV from Tauc plot that was much lower than that of the bulk counterpart due to the existence of defect states located in the band gap region. The performance of removal of heavy metal ions was examined by a batch-adsorption technique. The removal of lead and cadmium ions from aqueous solutions was rapid and efficient. It was found to be 98% and 85% for Pb(II) ion and Cd(II) ion respectively. The adsorption isotherms were determined by using Langmuir isotherm and the maximum absorption capacity was identified 6.3 mg/g and 1.8 mg/g for Pb(II) ion and Cd(II) ion respectively for 10 ppm solution respectively. Therefore, the wide bandgap Al_2O_3 nanoparticles could be a potential candidate for a variety of electronic and environmental applications.

Acknowledgments

The authors thankfully acknowledge the supports of Wazed Miah Science Research Centre (WMSRC), Jahangirnagar University, and Ms. Rabeya Akter Rabu acknowledges the National Science and Technology (NST) Fellowship, Ministry of Science and Technology, Government of the People's Republic of Bangladesh, for their financial support during this work..

References

1. Das R, Pachfule P, Banerjee R, Poddar P (2011) Metal and metal oxide nanoparticle synthesis from metal organic frameworks. Nanoscale 4: 591-599.
2. Nirmala TS, Iyandurai N, Yuvaraj S, Sundararajan M (2020) Effect of Cu^{2+} ions on structural, morphological, optical and magnetic behaviors of $ZnAl_2O_4$ spinel. Mater Res Express 7: 046104.
3. Kelgenbaeva Z, Khandaker JI, Ihara H, Omurzak E, Sulaimankulova S, et al. (2018) Thermal and optical properties of In and In_2O_3 nanoparticles synthesized using pulsed plasma in water. Phys Status Solidi A 215: 1700910.
4. Poursani AS, Nilchi A, Hassani A, Shariat SM, Nouri J (2016) The synthesis of nano TiO_2 and its use for removal of lead ions from aqueous solution. J Wat Resour Prot 8: 438-448.
5. Mousavand T, Takami S, Umetsu M, Ohara S, Adschiri T (2006) Supercritical hydrothermal synthesis of organic-inorganic hybrid nanoparticles. J Mater Sci 41: 1445-1448.
6. Ravindhranath K., Ramamoorty M (2017) Nano aluminium oxides as adsorbents in water remediation methods: A review. Rasayan J Chem 10: 716-722.
7. Ossman ME (2017) Similarity removal of heavy metals from aqueous solutions using advanced materials, with emphasis of synthetic and nanomaterials. Water Desalin Res J 1:1-44.
8. Ali S, Abbas Y, Zuhra Z, Butlerc IS (2018) Synthesis of g-alumina (Al_2O_3) nanoparticles and their potential for use as an adsorbent in the removal of methylene blue dye from industrial wastewater. Nanoscale Adv 1: 213-218.
9. Buzea C, Pacheco II, Robbie K (2007) Nanomaterials and nanoparticles: Sources and toxicity. Biointerphases 2. 2: 1934-8360.
10. Saleh TA, Gupta VK (2012) Synthesis and characterization of alumina nanoparticles polyamide membrane with enhanced flux rejection performance. Sep Purif Technol 89: 245-251.
11. Nuengmatcha P, Mahachai R, Chanthai S (2016) Adsorption capacity of the As-synthetic graphene oxide for the removal of alizarin red S dye from aqueous solution. Orient J Chem 32: 1399-1410.
12. Adschiri T, Hakuta Y, Arai K (2017) Hydrothermal synthesis of metal oxide fine particles at supercritical conditions. Ind Eng Chem Res 39: 4901-4907.
13. Ayusoa EA, Sanchezb AG, Querola X (2007) Adsorption of Cr(VI) from synthetic solutions and electroplating wastewaters on amorphous aluminium oxide. J Hazard Mater 142: 191-198.
14. Neouze MA, Schubert U (2008) Surface modification and functionalization of metal and metal oxide nanoparticles by organic ligands. Monatsh Chem 139: 183-195.
15. Aparicio M, Pellice SA, Dura A, Rosero-Navarro NC (2008) Effects of Ce-containing Sol-gel coatings reinforced with Sio_2 nanoparticles on the protection of AA20204. Corros Sci 50: 1283-1291.
16. Farahmandjou M, Golabiyan N (2019) Synthesis and characterization of Al_2O_3 nanoparticles as catalyst prepared by polymer co-precipitation method. Mater Eng Res 1: 40-44.
17. Sharma YC, Srivastava V, Upadhyay SN, Weng, CH (2008) Alumina nanoparticles for the removal of Ni(II) from aqueous solutions. Ind Eng Chem 47: 8095-8100.
18. Parida KM, Amaresh CP, Das J, Nruparaj S (2009) Synthesis and characterization of nano-sized porous gamma-alumina by control precipitation method. Mater Chem Phys 113: 244-248.
19. Zhou S, Antonietti M, Niederberger M (2007). Low temperature synthesis of alumina nano crystals from aluminium acetylacetonate in nonaqueous media. Small 3: 763-767.

20. Tang B, Ge J, Zhuo L, Wang G, Niu J, et al. (2005) A facile and controllable synthesis of alumina nanostructure without a surfactant. Eur J Inorg Chem 2005: 4366-4369.

21. Siengchin S, Karger-Kociss J, Thomann R (2007) Alumina-filled polystyrene micro- and nanocomposites prepared by melt mixing with and without latex precompounding: Structure and properties. J Appl Polym Sci 105: 2963-2972.

22. Reddy BSB, Das K, Das S (2007) A review on synthesis of *in situ* Aluminium based composites by thermal, mechanical and mechanical-thermal activation of chemical reactions. J Mater Sci 42: 9366-9378.

23. Kaya C, H JY, Gu X, Butler EG (2002) Nanostructured ceramic powders by hydrothermal synthesis and their applications. Micropor Mesopor Mat 54: 37-49.

24. Sundararajan M, Kennedy LJ (2017) Photocatalytic removal of rhodamine B under irradiation of visible light using $Co_{1-x}Cu_xFe_2O_4$ ($0 \leq x \leq 0.5$) nanoparticles. J Env Chem Eng 5: 4075-4092.

25. Bujdák J, Rode BM (2003) Alumina catalyzed reactions of amino acids. J Thermal Anal Calorim 73: 797-805.

26. Banerjee S, Dubey S, Gautam RK, Chattopadhyaya MC, Sharma YC (2019) Adsorption characteristics of alumina nanoparticles for the removal of hazardous dye, orange G from aqueous solutions. Arab J Chem 12: 5339-5354.

27. Bahlawane N, Watanabe T (2000) New sol-gel route for the preparation of pure alumina at 950°C. J Am Ceram Soc 83: 2324-2326.

Author Affiliation

Top

[1]*Department of Physics, Jahangirnagar University, Savar, Dhaka, 1342, Bangladesh*

[2]*Department of Chemistry, Jahangirnagar University, Savar, Dhaka, 1342, Bangladesh*

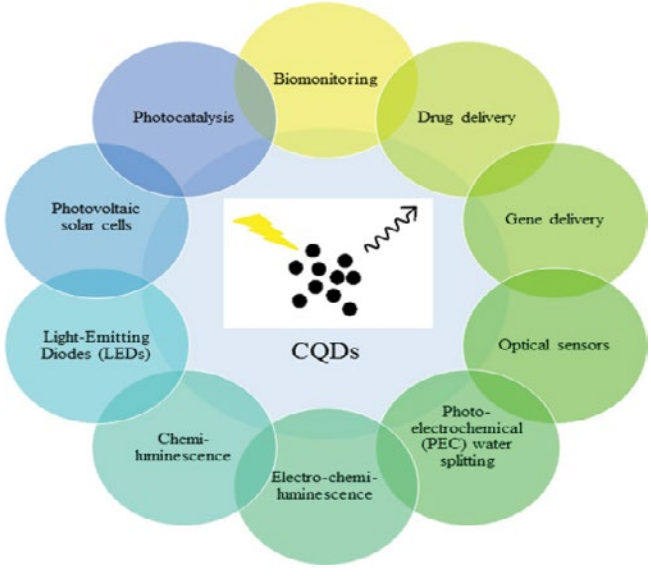

Figure 5: Various applications of carbon dots.

Citation: *Rabu1 RA, Jewena N, Das SK, JI Khandaker, Ahmed F. (2020) Synthesis of Metal-Oxide (Al2O3) Nanoparticles by using Autoclave for the Efficient Absorption of Heavy Metal Ions. J Nanomater Mol Nanotechnol 9:6.*